The Astrophysical Journal, 802:36 (9pp), 2015 March 20 doi:10.1088/0004-637X/802/1/36


# NON-LTE ANALYSIS OF NEUTRAL COPPER IN LATE-TYPE METAL-POOR STARS*

H. L. Yan[1,2], J. R. Shi[1], and G. Zhao[1]
[1] Key Laboratory of Optical Astronomy, National Astronomical Observatories, Chinese Academy of Sciences, Beijing 100012, China; sjr@nao.cas.cn
[2] University of Chinese Academy of Sciences, Beijing 100049, China
*Received 2014 October 19; accepted 2015 January 15; published 2015 March 18*

## ABSTRACT

We investigated the copper abundances of 64 late-type stars in the Galactic disk and halo with effective temperatures from 5400 to 6700 K and [Fe/H] from −1.88 to −0.17. For the first time, the copper abundances are derived using both local thermodynamic equilibrium (LTE) and non-local thermodynamic equilibrium (non-LTE) calculations. High-resolution ($R > 40{,}000$), high signal-to-noise ratio (S/N > 100) spectra from the FOCES spectrograph are used. The atmospheric models are calculated based on the MAFAGS opacity sampling code. All the abundances are derived using spectrum synthesis methods. Our results indicate that the non-LTE effects of copper are important for metal-poor stars, showing a departure of ∼0.17 dex at a metallicity of $\sim -1.5$. We also find that the copper abundances derived from non-LTE calculations are enhanced compared with those from LTE. The enhancements show clear dependence on the metallicity, which gradually increases with decreasing [Fe/H] for our program stars, leading to a flatter distribution of [Cu/Fe] with [Fe/H] than previous work. There is a hint that the thick- and thin-disk stars have different behaviors in [Cu/Fe], and bending of the disk stars may exist.

*Key words:* Galaxy: evolution – line: formation – line: profiles – stars: abundances – stars: late-type

## 1. INTRODUCTION

Investigation of elemental abundances traces the evolution of the Galaxy. The chemical history of the Galaxy is dominated by the processes of nucleosynthesis in each generation of stars. Based on the observational behaviors of elemental abundances in stars with different metallicities, one can not only look back at the Galactic chemical enrichment history, but also constrain the theoretical evolutionary models of our Galaxy. Copper is of particular interest among the iron-peak elements because, first, it has a unique evolutionary trend as the [Fe/H] varies from extremely metal-poor to the solar abundance, and second, this element is thought to be synthesized by several possible nucleosynthesis scenarios, yet the contributions of these scenarios are still in dispute.

From an observational point of view, although it was Cohen (1978, 1979, 1980) who gave an early look at the Galactic copper abundances (they investigated 27 red giants in 7 globular clusters) and who first suggested a decreasing trend of [Cu/Fe] with decreasing [Fe/H], the evolutionary trend of [Cu/Fe] was not established firmly until Sneden et al. (1991). In a series of works (Gratton & Sneden 1988; Sneden & Crocker 1988; Sneden et al. 1991), the authors derived the copper abundances for a large sample of stars in the Galactic disk and halo. Their results clearly showed a linear trend of [Cu/Fe], which increases toward higher metallicity. This trend was partly confirmed by Mishenina et al. (2002) and Simmerer et al. (2003); the former authors investigated an expanded sample of disk and halo stars with a wide range of metallicities, while the latter managed to measure the copper abundances of 117 giants in 10 globular clusters. Furthermore, both works indicated a flat plateau of [Cu/Fe] at the metal-poor end, which is roughly [Cu/Fe] $\approx -0.75$ at [Fe/H] $< -1.5$. Some contemporaneous studies on single ultra-metal-poor stars seemed consistent with this flat distribution (e.g., Westin et al. 2000; Cowan et al. 2002; Sneden et al. 2003). However, using near-UV lines, Bihain et al. (2004) and Lai et al. (2008) suggested the plateau should be around −1 instead of −0.75. Reddy et al. (2003, 2006) investigated a large sample of disk stars, and they found little variation of [Cu/Fe] with [Fe/H] in the metallicity range [Fe/H] $> -0.8$, where the values of [Cu/Fe] show no evident divergence with respect to the solar copper abundance. Thus, a slight S-shape of [Cu/Fe] as a function of [Fe/H] can be seen by overlapping data from different authors (Bihain et al. 2004, Figure 1). Although the stars investigated as part of a great quantity of work followed the Galactic general S-shape (e.g., Prochaska et al. 2000; Shetrone et al. 2001, 2003; Cohen et al. 2008; Mishenina et al. 2011), several peculiar structures were still detected, such as the Ursa Major moving Group (UMaG; Castro et al. 1999), Omega Centauri ($\omega$ Cen; Smith et al. 2000; Cunha et al. 2002), Sagittarius dwarf spheroidal galaxy (Sgr dSph; McWilliam & Smecker-Hane 2005; McWilliam et al. 2013), and the halo subpopulation (Nissen & Schuster 2011). Their discordant trends of [Cu/Fe] may imply different chemical evolutionary histories with respect to our Milky Way.

Theoretically, copper is thought to be produced in multiple astrophysical sites. The first one is the weak *s*-process, which takes place in massive stars during the helium- and carbon-shell burning stage (Sneden et al. 1991). It is a secondary process that needs iron seeds from previous generations of stars, resulting in the linear dependence of [Cu/Fe] on [Fe/H]. Bisterzo et al. (2004) proposed a revised version of this scenario, suggesting *sr*− process dominated copper synthesis in massive stars instead of classical *s*-process. Additionally, simulations of Galactic chemical evolution (GCE) by Romano & Matteucci (2007) and Romano et al. (2010) also support that massive stars contribute most of the copper. However, Matteucci et al. (1993) showed the second possibility by fitting GCE models to interpret observational data. They suggested that the main source of copper was Type Ia supernovae (SNe Ia) instead of *s*-process (but they needed to increase the yields from SNe Ia by about an order of magnitude). This conclusion was subsequently supported by

* Based on observations collected at the Germany–Spanish Astronomical Center, Calar Alto, Spain.

the work of Mishenina et al. (2002) and Simmerer et al. (2003). The third mechanism comes from the constraint of the [Cu/Fe] plateau at low metallicity, which requires contributions from primary explosive nucleosynthesis in Type II supernovae (SNe II; e.g., Timmes et al. 1995). However, the productions calculated from SNe II are model-dependent (Woosley & Weaver 1995; Kobayashi et al. 2006; Nomoto et al. 2006; Romano et al. 2010), resulting in discordant predicted fractions. Besides, large scatter in observational results also plays a relevant role (see the examples given by Pignatari et al. 2010). The last source was the main *s*-process operating in low- and intermediate-mass AGB stars, which was thought to contribute only about 5% of the solar copper (Travaglio et al. 2004).

So far, a number of analyses on copper abundance have been presented, covering the whole range of metallicity from solar to the most extreme metal-poor stars, but none of them were carried out with non-local thermodynamic equilibrium (non-LTE) calculations. This is partly because non-LTE calculations need a reliable atomic model and detailed statistical equilibrium calculations, neither of which is a simple job for copper. Despite the difficulties, there are at least two principal reasons that we have to put non-LTE analysis into perspective. First, recent studies on non-LTE effects have demonstrated that the non-LTE correction is large for some elements in metal-poor stars (e.g., Baumueller & Gehren 1997; Zhao et al. 1998; Zhao & Gehren 2000; Gehren et al. 2004; Shi et al. 2004, 2009; Bergemann & Gehren 2008). Moreover, only a few lines can be used to perform copper abundance analysis when dealing with metal-poor stars with relatively higher temperatures, as there is little neutral copper in the atmospheres of such stars. The analysis has to rely on the two resonance lines at 3247 and 3273 Å, both of which may suffer large non-LTE effects (Roederer et al. 2012, 2014). Bihain et al. (2004) and Bonifacio et al. (2010) also reported that the abundances derived from these two lines are inconsistent with those derived from other optical Cu I lines.

In this paper, we aim to explore the copper abundances for the sample stars in the metallicity range $-1.88 <$ [Fe/H] $< -0.17$ with a complete spectrum synthesis method based on the population level calculated from the statistical equilibrium equations. In Section 2, we will briefly introduce some key information about the observations. The fundamental work for the abundance analysis, i.e., the atmospheric model, stellar parameters, and atomic line data are presented in Section 3. Section 4 will provide details of non-LTE calculations, including the atomic model. In Section 5 we will show the final results and error analysis. The discussions and conclusions are presented in Sections 6 and 7, respectively.

## 2. OBSERVATIONS

The sample stars investigated in this paper have already been discussed by Gehren et al. (2004, 2006). Here, we simply list the key features of the sample and the observations. More details can be found in the aforementioned papers.

1. The observations were carried out on the 2.2 m telescope located at Calar Alto Observatory over the years 1999–2003. The FOCES échelle spectrograph was used to obtain high-resolution spectra, providing 97 spectral orders in total that started at 3700 Å and ended at 9800 Å.
2. The detector was a CCD chip with 2048 × 2048 pixels, and the size for each pixel is 24 $\mu$m. A two-pixel bin results in a ~40,000 resolution power ($R$).
3. The total exposure time is divided into more than two exposures. The final combined spectra show a signal-to-noise ratio (S/N) that is higher than 100.
4. The spectra were reduced with the program designed for the FOCES spectrograph (Pfeiffer et al. 1998), which worked under the IDL environment. Cosmic rays and bad pixels were removed by careful comparisons of exposures from the same object. The instrumental response and background light scatter were also considered during the data reduction.

## 3. FUNDAMENTAL WORK FOR ABUNDANCE ANALYSIS

In this section, we briefly describe the methods and key information our studies are based on, including the atmospheric model, the determinations of stellar parameters, the atomic line data, and the kinematic properties of our program stars.

### 3.1. Model Atmosphere

The stellar atmospheric model is the foundation of the spectrum synthesis. Our work adopted the MAFAGS opacity sampling (OS) model. This code was developed by Grupp (2004) and updated by Grupp et al. (2009) with the new iron atomic data computed by Kurucz (2009). The MAFAGS OS code describes a one-dimensional plane-parallel model with 80 layers overall in the hydrostatic equilibrium state. Chemical homogeneity and local thermal equilibrium are assumed throughout the atmosphere. This model atmosphere was also applied in our previous work (Mashonkina et al. 2011; Shi et al. 2014).

The comparison between the MAFAGS and MARCS OS model was performed by Shi et al. (2014). Although differences in the temperatures between those two models exist outside $\log \tau \simeq -4$ and inside $\log \tau \simeq 0.3$, both of these regions barely influence the synthetic copper spectral line profile.

### 3.2. Stellar Parameters

For all of our program stars, we directly adopted the stellar parameters derived by Gehren et al. (2004, 2006). By fitting the theoretical profiles to the observational data, two Balmer lines were used to derive the effective temperatures ($T_{\rm eff}$). The hydrogen broadening theory involved in the theoretical profile calculation was from Ali & Griem (1966). The surface gravities ($\log g$) were obtained with $[g] = [\mathrm{Mass/Luminosity}] + 4[T_{\rm eff}]$, where the stellar mass and luminosity were evaluated with the help of evolutionary tracks (VandenBerg et al. 2000) and HIPPARCOS parallaxes. In addition, the microturbulence velocities ($\xi$) were determined simultaneously with the metallicities ([Fe/H]): the [Fe/H] determined from the Fe II line is supposed to be independent of the equivalent width. The final uncertainties in $T_{\rm eff}$, $\log g$, [Fe/H], and $\xi$ were estimated to be $\pm 80$ K, $\pm 0.05$ dex, $\pm 0.05$ dex, and $\pm 0.1$ km s$^{-1}$, respectively.

**Table 1**
Atomic Data of Copper Lines Used in this Work

| $\lambda_{air}$ (Å) | Transition | $E_{low}$ (eV) | log $gf$ | log $C_6$ |
|---|---|---|---|---|
| 5105.541 | $4s^2\,^2D_{5/2}-4p\,^2P^o_{3/2}$ | 1.389 | −1.64 | −31.67 |
| 5218.202 | $4p\,^2P^o_{3/2}-4d\,^2D_{5/2}$ | 3.817 | +0.28 | −30.57 |
| 5782.132 | $4s^2\,^2D_{3/2}-4p\,^2P^o_{1/2}$ | 1.642 | −1.89 | −31.66 |

**Notes.** The log $gf$ values were rectified from the non-LTE solar spectrum fitting, and the van der Waals damping constants (log $C_6$) were calculated according to Anstee & O'Mara (1991, 1995).

### 3.3. Atomic Line Data

We used a set of calibrated log $gf$ values, each of which could reproduce the solar copper abundance independently, as presented by Shi et al. (2014). Furthermore, the van der Waals damping constants (log $C_6$) for Cu I were calculated according to Anstee & O'Mara (1991, 1995). Five Cu I lines can be seen in our FOCES spectra. For the evaluation of copper abundance, 5220.070 and 5700.240 Å are not good indicators, as both of them are badly blended in most of our program stars. As a result, the remaining three lines are applied to our research, which are 5105.541, 5218.202, and 5782.132 Å. The atomic line data of the three lines are listed in Table 1.

### 3.4. Population and Kinematic Properties

Similar to the stellar parameters, we also adopted the population identified by Gehren et al. (2004, 2006) for our program stars, which was based on the kinematic features, stellar ages, and [Al/Mg] and [Mg/Fe] ratios. Most of the stars were classified as thin-disk, thick-disk, and halo population, whereas the rest were stars with peculiarities.

## 4. NON-LTE CALCULATIONS

LTE assumption provides us a simple way to calculate the population of each energy level and number densities of different ionization stages for a given element, while non-LTE calculations require solving the detailed statistical equilibrium equations. Thus, a reliable atomic model of copper is indispensable.

The atomic model of copper has been described in the previous paper (Shi et al. 2014) and the Grotrian diagram of the model can also be seen there. We modeled the copper atom with 17 orbits, 97 energy levels (96 states for Cu I and the ground state for Cu II), and 1089 transitions, and the fine structure for the levels with low excitation energy was also included. The atomic data of such complex structures are obtained from both laboratory measurements (NIST[3] database, Sugar & Musgrove 1990) and theoretical calculations (Liu et al. 2014). In addition, the excitation and ionization caused by inelastic collisions were also considered. The data for collisions with neutral hydrogen were obtained based on the Drawin formula (Drawin 1968, 1969) presented by Steenbock & Holweger (1984), and we decreased the collisional rates by an order of magnitude ($S_H = 0.1$) under the suggestion of Shi et al. (2014). The excitation and ionization caused by inelastic collisions with electrons are calculated according to a number of theoretical works (van Regemorter 1962; Seaton 1962; Allen 1973). We used a revised DETAIL program (Butler & Giddings 1985) with an accelerated lambda iteration method to perform the statistical equilibrium calculations.

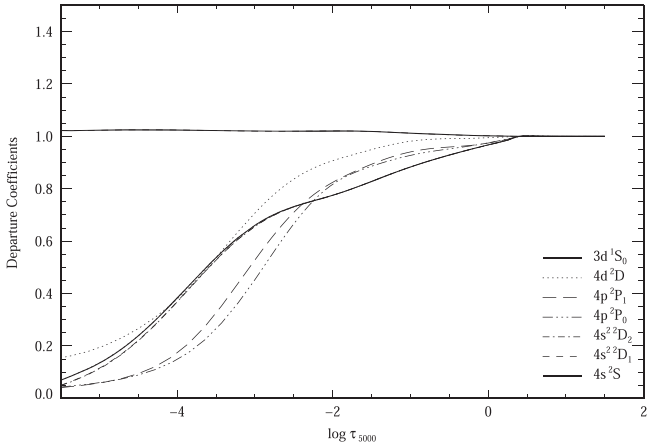


**Figure 1.** Departure coefficients ($b_i$) for selected energy levels (listed in the figure) as a function of continuum optical depth at 5000 Å for the model atmosphere of HD 59984. The collision with neutral hydrogen was scaled by a factor of 0.1 in light of Shi et al. (2014).

In Figure 1, we present how the departure coefficients ($b_i = n_i^{\text{non-LTE}}/n_i^{\text{LTE}}$) of the selected levels vary with the continuum optical depth at 5000 Å (log $\tau_{5000}$) for the model atmosphere of HD 59984 , where $b_i$ is the ratio of the number density of non-LTE ($n_i^{\text{non-LTE}}$) to that of LTE ($n_i^{\text{LTE}}$). HD 59984 is a typical star with moderate temperature and metallicity among our sample, and is randomly selected as an example for the convenience of discussion. The departure coefficients for important levels of Cu I and the Cu II ground state are shown in the figure. It also shows that the number densities of these levels begin to underpopulate outside layers with log $\tau_{5000} \sim 0.5$ due to overionization.

## 5. RESULTS

### 5.1. Spectral Line Synthesis

In our analysis, transitions of the hyperfine structure (HFS) were calculated according to Biehl (1976) with the RS coupling method. For the lines we used, if the intervals of HFS components are within 1 mÅ, we combined them. The adopted solar copper abundance is the value derived from the meteorites, which is log $\varepsilon_\odot$(Cu) = 4.25 (Lodders et al. 2009), and the oscillator strengths were also calibrated based on this value as described in the aforementioned section. Additionally, the ratio between two copper isotopes ($^{63}$Cu and $^{65}$Cu) was assumed to be 0.69:0.31 (Asplund et al. 2009). An IDL-based program, SIU, was used to perform the line formation in our abundance determinations, which was developed by Reetz (1991). In our analysis, the broadenings caused by the macroturbulence, rotation, and instrument were treated as one single Gauss broadening factor being convolved with the synthetic spectra to fit the observed line profile. The comparison between the synthetic and observed line profiles at 5105 Å for HD 59984 is shown in Figure 2 as an example. The observed spectrum and theoretical synthesis are represented by filled circles and the solid line, respectively. The uncertainty of our line profile synthesis is less than 0.02 dex.

[3] http://www.physics.nist.gov/

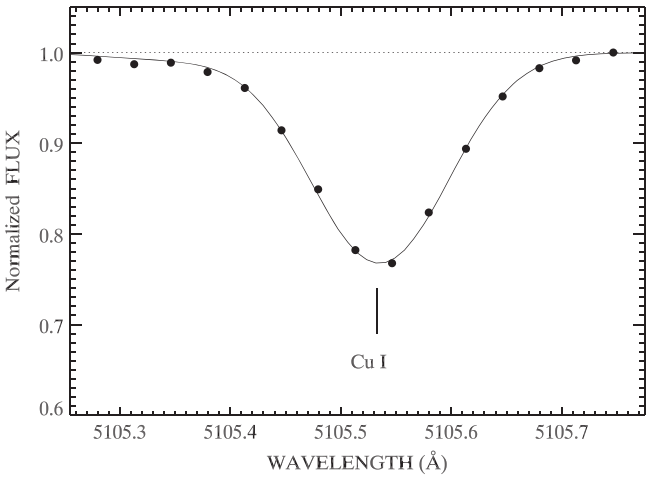


**Figure 2.** Synthetic profile of the Cu I 5105 Å line for HD 59984. The observed spectrum and theoretical synthesis are represented by filled circles and the solid line, respectively.

### 5.2. Copper Abundances and Error Analysis

The copper abundances are derived successfully for 60 stars in our sample, and the selected Cu I lines are too weak to rely on for the remaining four stars, which are HD 241253, HD 233511, G 119–32, and BD +20° 2594. The derived abundances with both LTE and non-LTE calculations are listed in Table 2, where the results of each individual line are also presented. The final abundance of each star is found by calculating the arithmetical mean value of every line used in the analysis.

The trend of [Cu/Fe] to [Fe/H] for our program stars is shown in Figure 3. The errors in the figure are evaluated by computing the standard deviations of the abundances derived from different spectral lines. Our results do not show a large abundance discrepancy between different lines. We present the errors as a function of [Fe/H] in Figure 4. In LTE calculations, the standard deviations vary from 0.01 to 0.11, slightly larger than those in non-LTE, which are between 0.01 and 0.08. Furthermore, the LTE standard deviations become large at the metal-poor end, while the non-LTE ones remain stable. Both of them have a mean value around 0.04. The errors caused by the uncertainties of the stellar parameters are estimated for HD 59984, and the resulting effects in [Cu/Fe] are ±0.07, <0.01, ±0.05, and <0.01 dex for the typical uncertainties in $T_{\rm eff}$, log $g$, [Fe/H], and $\xi$, respectively.

The differences in [Cu/Fe] between non-LTE and LTE for our program stars as a function of metallicity, effective temperature, and surface gravity are plotted in Figure 5. The non-LTE departure shows clear dependence on the metallicity (see Figure 5(a)), which gradually increases as [Fe/H] decreases in our program stars.

### 5.3. Non-LTE Effects

The final results in Table 2 show that the abundances derived from non-LTE calculations are larger than those from LTE ones for our program stars. The non-LTE correction for an individual spectral line can reach ∼+0.20 dex for stars with [Fe/H] ∼ −1.5. The increase in copper abundance in the non-LTE calculation is a consequence of the underpopulation of the lower energy levels ($4s^2\,^2D$ and $4p\,^2P^o$), as shown in Figure 1. This deviation will lead to a underestimation of the copper abundance with LTE analysis.

For each Cu I line, the non-LTE effect is different, reflecting the properties of corresponding energy levels and associated transitions. The lines of 5105 and 5782 Å exhibit larger non-LTE effects compared with the weaker 5218 Å. Taking HD 59984 as an example again, the non-LTE corrections for the 5105 and 5782 Å lines are 0.10 and 0.09 dex, respectively, and 0.06 dex for the weaker 5218 Å line. On one hand, despite the 5218 Å line suffering fewer non-LTE effects than the other ones, it is usually blended by the 5217 Å line (Fe II line), and thus it is not a satisfactory indicator of stars with low or moderate metallicity. On the other hand, since most abundance analyses are based on the two copper strong lines, one needs to be aware of the non-LTE departures, especially for metal-poor stars.

### 5.4. Comparison with Other Work

A number of studies of copper abundance have been carried out so far, allowing us to compare our results with those derived by several different groups based on LTE calculations. Compared with work published in recent years, we found 47 stars in common (11 of them are studied at least twice in different papers). In Figure 6, we compare our results derived from LTE calculations with those in other works. In general, the LTE [Cu/Fe] values determined in our work are consistent with the different studies presented here, and no clear systematic deviation is found. We briefly discussed the details of the comparisons and the possible reasons for the large scatter.

*Mishenina et al. (2002, 2011).* Mishenina et al. (2002) studied copper abundances for 90 metal-poor stars in the year 2002, and in 2011 they investigated 172 F–K dwarf stars and derived their copper abundances. All their observations were performed with $R$ = 42,000 and S/N > 100. The copper abundances were derived from the 5105, 5218, and 5782 Å lines, which are the same as those in our studies. The oscillator strengths adopted in their studies were from Gurtovenko & Kostyk (1989). We have 13 stars in common, and 4 of them are investigated in both of their papers. Since the derived [Cu/Fe] of these four stars varied a little bit for their two papers, we therefore adopted the latest values (derived in 2011) to perform the comparison. The resulting average difference of the 13 stars is $\Delta$[Cu/Fe] = −0.01 ± 0.12. The main contribution to the relatively large scatter is from four stars, namely HD 22879, HD 101177, HD 108076, and HD 218209, as the [Cu/Fe] values derived in our work and theirs differ by more than 0.1 dex for those stars. This is mainly due to the differences in the stellar parameters adopted in the two studies.

*Reddy et al. (2003, 2006).* The authors performed an abundance analysis on a large sample of F and G dwarfs, containing thin-/thick-disk and halo stars. The copper abundances were determined from the 5105 Å, 5218 Å, and 5220 Å lines. Their log $gf$ values are similar to ours. From their samples, 21 stars are found in common with ours, and the mean difference is $\Delta$[Cu/Fe] = 0.01 ± 0.10. Most of the stars show no large deviation except HD 200580 and HD 107582. The [Fe/H] values for these two stars adopted in their studies are different from those in ours. Taking [Fe/H] variances into account, the deviation can be perfectly removed.

*Allende Prieto et al. (2004).* These authors analyzed a complete and comprehensive sample of 118 stars with absolute

**Table 2**
Copper Abundances of our Program Stars

| Star | $T_{\rm eff}$ | log $g$ | [Fe/H] | $\xi$ | 5105 Å | 5218 Å | 5782 Å | [Cu/Fe] | POP | LinFor |
|---|---|---|---|---|---|---|---|---|---|---|
| HD 17948 | 6325 | 4.13 | −0.35 | 1.90 | −0.25 | −0.19 | −0.16 | −0.20 ± 0.05 | D | L |
| | | | | | −0.18 | −0.13 | −0.09 | −0.13 ± 0.05 | | N |
| HD 22309 | 5900 | 4.29 | −0.31 | 1.30 | 0.03 | −0.04 | −0.03 | −0.01 ± 0.04 | D | L |
| | | | | | 0.07 | −0.02 | 0.01 | 0.02 ± 0.05 | | N |
| HD 22879 | 5775 | 4.26 | −0.83 | 1.10 | −0.25 | −0.13 | −0.15 | −0.18 ± 0.06 | T | L |
| | | | | | −0.17 | −0.10 | −0.08 | −0.12 ± 0.05 | | N |
| HD 30649 | 5765 | 4.26 | −0.58 | 1.10 | 0.03 | 0.03 | 0.02 | 0.03 ± 0.01 | T | L |
| | | | | | 0.09 | 0.05 | 0.07 | 0.07 ± 0.02 | | N |
| HD 243357 | 5675 | 4.38 | −0.59 | 1.10 | −0.04 | 0.05 | −0.02 | 0.00 ± 0.05 | T | L |
| | | | | | 0.01 | 0.07 | 0.03 | 0.04 ± 0.03 | | N |
| HD 36283 | 5475 | 4.28 | −0.41 | 0.80 | 0.01 | 0.13 | 0.05 | 0.06 ± 0.06 | T | L |
| | | | | | 0.04 | 0.13 | 0.08 | 0.08 ± 0.05 | | N |
| G 99–21 | 5525 | 4.30 | −0.63 | 1.00 | −0.13 | 0.01 | −0.10 | −0.07 ± 0.07 | T | L |
| | | | | | −0.09 | 0.03 | −0.06 | −0.04 ± 0.06 | | N |
| HD 250792 | 5600 | 4.32 | −1.02 | 1.10 | −0.38 | −0.40 | −0.38 | −0.39 ± 0.01 | H | L |
| | | | | | −0.30 | −0.38 | −0.31 | −0.33 ± 0.04 | | N |
| HD 46341 | 5880 | 4.36 | −0.58 | 1.80 | −0.05 | −0.07 | −0.08 | −0.07 ± 0.02 | T | L |
| | | | | | 0.01 | −0.04 | −0.02 | −0.02 ± 0.03 | | N |
| HD 56513 | 5630 | 4.53 | −0.45 | 1.20 | −0.06 | −0.01 | 0.01 | −0.02 ± 0.04 | D | L |
| | | | | | −0.03 | 0.00 | 0.04 | 0.00 ± 0.04 | | N |
| HD 58551 | 6190 | 4.23 | −0.53 | 1.80 | −0.13 | −0.07 | −0.02 | −0.07 ± 0.06 | D | L |
| | | | | | −0.05 | −0.01 | 0.06 | 0.00 ± 0.06 | | N |
| HD 59374 | 5840 | 4.37 | −0.83 | 1.40 | −0.16 | −0.17 | −0.08 | −0.14 ± 0.05 | T | L |
| | | | | | −0.08 | −0.13 | 0.00 | −0.07 ± 0.07 | | N |
| HD 59984 | 5925 | 3.94 | −0.74 | 1.20 | −0.12 | −0.06 | −0.08 | −0.09 ± 0.03 | T | L |
| | | | | | −0.02 | 0.00 | 0.01 | 0.00 ± 0.02 | | N |
| HD 60319 | 5875 | 4.17 | −0.82 | 1.40 | −0.15 | −0.10 | −0.15 | −0.13 ± 0.03 | T | L |
| | | | | | −0.06 | −0.05 | −0.06 | −0.06 ± 0.01 | | N |
| G 235–45 | 5500 | 4.25 | −0.59 | 1.10 | 0.01 | −0.01 | 0.05 | 0.02 ± 0.03 | T | L |
| | | | | | 0.05 | 0.00 | 0.09 | 0.05 ± 0.05 | | N |
| HD 88446 | 5915 | 4.03 | −0.44 | 1.60 | −0.01 | −0.08 | −0.14 | −0.08 ± 0.07 | D | L |
| | | | | | −0.04 | −0.04 | −0.07 | −0.05 ± 0.02 | | N |
| HD 88725 | 5665 | 4.35 | −0.70 | 1.20 | −0.01 | 0.03 | 0.03 | 0.02 ± 0.02 | T | L |
| | | | | | 0.05 | 0.06 | 0.09 | 0.07 ± 0.02 | | N |
| HD 91784 | 5890 | 4.47 | −0.33 | 1.30 | −0.01 | 0.06 | 0.06 | 0.04 ± 0.04 | D | L |
| | | | | | 0.03 | 0.08 | 0.10 | 0.07 ± 0.04 | | N |
| HD 94028 | 5925 | 4.19 | −1.51 | 1.50 | −0.57 | −0.41 | ⋯ | −0.49 ± 0.11 | H | L |
| | | | | | −0.37 | −0.28 | ⋯ | −0.32 ± 0.06 | | N |
| HD 96094 | 5900 | 4.01 | −0.46 | 1.70 | −0.05 | −0.06 | 0.01 | −0.03 ± 0.04 | D | L |
| | | | | | 0.02 | −0.02 | 0.07 | 0.02 ± 0.05 | | N |
| HD 97855*A* | 6240 | 4.13 | −0.44 | 1.80 | −0.22 | −0.15 | −0.11 | −0.16 ± 0.06 | D | L |
| | | | | | −0.14 | −0.09 | −0.03 | −0.09 ± 0.06 | | N |
| HD 101177 | 5890 | 4.30 | −0.47 | 1.80 | 0.09 | 0.04 | 0.14 | 0.09 ± 0.05 | D | L |
| | | | | | 0.16 | 0.07 | 0.20 | 0.14 ± 0.07 | | N |
| HD 104056 | 5875 | 4.31 | −0.41 | 1.30 | −0.02 | 0.00 | 0.02 | 0.00 ± 0.02 | D | L |
| | | | | | 0.03 | 0.02 | 0.06 | 0.04 ± 0.02 | | N |
| HD 107582 | 5565 | 4.34 | −0.61 | 1.00 | −0.10 | −0.09 | −0.15 | −0.11 ± 0.03 | T | L |
| | | | | | −0.06 | −0.07 | −0.11 | −0.08 ± 0.03 | | N |
| HD 108076 | 5725 | 4.44 | −0.73 | 1.20 | −0.20 | −0.17 | −0.21 | −0.19 ± 0.02 | D | L |
| | | | | | −0.14 | −0.15 | −0.16 | −0.15 ± 0.01 | | N |
| HD 114606 | 5610 | 4.28 | −0.57 | 1.20 | 0.04 | 0.06 | 0.02 | 0.04 ± 0.02 | T | L |
| | | | | | 0.09 | 0.08 | 0.06 | 0.08 ± 0.02 | | N |
| HD 118659 | 5510 | 4.36 | −0.60 | 1.00 | −0.03 | 0.01 | 0.02 | 0.00 ± 0.03 | T | L |
| | | | | | 0.02 | 0.02 | 0.06 | 0.03 ± 0.02 | | N |
| HD 119288 | 6420 | 4.13 | −0.17 | 1.90 | −0.34 | ⋯ | −0.26 | −0.30 ± 0.06 | D | L |
| | | | | | −0.28 | ⋯ | −0.20 | −0.24 ± 0.06 | | N |
| HD 123710 | 5790 | 4.41 | −0.54 | 1.40 | 0.07 | 0.08 | 0.06 | 0.07 ± 0.01 | D | L |
| | | | | | 0.13 | 0.11 | 0.11 | 0.12 ± 0.01 | | N |
| HD 126512 | 5825 | 4.02 | −0.64 | 1.60 | −0.03 | 0.02 | 0.06 | 0.02 ± 0.05 | T | L |
| | | | | | 0.05 | 0.07 | 0.14 | 0.09 ± 0.05 | | N |
| HD 134169 | 5930 | 3.98 | −0.86 | 1.80 | 0.01 | −0.04 | ⋯ | −0.02 ± 0.04 | T | L |
| | | | | | 0.13 | 0.04 | ⋯ | 0.09 ± 0.06 | | N |
| HD 142267 | 5807 | 4.42 | −0.46 | 1.00 | 0.01 | −0.06 | −0.02 | −0.02 ± 0.04 | D | L |
| | | | | | 0.06 | −0.04 | 0.02 | 0.01 ± 0.05 | | N |

**Table 2**
(Continued)

| Star | $T_{\rm eff}$ | log $g$ | [Fe/H] | $\xi$ | 5105 Å | 5218 Å | 5782 Å | [Cu/Fe] | POP | LinFor |
|---|---|---|---|---|---|---|---|---|---|---|
| HD 144061 | 5815 | 4.44 | −0.31 | 1.20 | 0.00 | −0.06 | 0.04 | −0.01 ± 0.05 | D | L |
| | | | | | 0.04 | −0.05 | 0.07 | 0.02 ± 0.06 | | N |
| HD 148816 | 5880 | 4.07 | −0.78 | 1.20 | −0.04 | −0.07 | −0.02 | −0.04 ± 0.03 | ? | L |
| | | | | | 0.06 | −0.02 | 0.07 | 0.04 ± 0.05 | | N |
| HD 149996 | 5665 | 4.09 | −0.52 | 1.20 | 0.00 | 0.08 | 0.00 | 0.03 ± 0.05 | T | L |
| | | | | | 0.06 | 0.11 | 0.05 | 0.07 ± 0.03 | | N |
| BD +68° 901 | 5715 | 4.51 | −0.25 | 1.40 | −0.12 | −0.14 | −0.04 | −0.10 ± 0.05 | D | L |
| | | | | | −0.09 | −0.13 | −0.01 | −0.08 ± 0.06 | | N |
| HD 157089 | 5800 | 4.06 | −0.59 | 1.20 | −0.08 | −0.09 | −0.05 | −0.07 ± 0.02 | T | L |
| | | | | | −0.01 | −0.06 | 0.01 | −0.02 ± 0.04 | | N |
| HD 157466 | 5990 | 4.38 | −0.44 | 1.10 | −0.20 | −0.22 | −0.15 | −0.19 ± 0.04 | D | L |
| | | | | | −0.14 | −0.20 | −0.10 | −0.15 ± 0.05 | | N |
| HD 158226 | 5805 | 4.12 | −0.56 | 1.10 | 0.04 | −0.03 | 0.04 | 0.02 ± 0.04 | T | L |
| | | | | | 0.11 | 0.00 | 0.10 | 0.07 ± 0.06 | | N |
| G 170−56 | 6030 | 4.31 | −0.79 | 1.30 | −0.42 | −0.29 | ⋯ | −0.35 ± 0.09 | ? | L |
| | | | | | −0.33 | −0.24 | ⋯ | −0.28 ± 0.06 | | N |
| HD 160933 | 5765 | 3.85 | −0.27 | 1.20 | −0.16 | −0.19 | −0.16 | −0.17 ± 0.02 | D | L |
| | | | | | −0.12 | −0.17 | −0.12 | −0.14 ± 0.03 | | N |
| HD 160693 | 5850 | 4.31 | −0.60 | 1.20 | 0.05 | 0.01 | 0.08 | 0.05 ± 0.04 | ? | L |
| | | | | | 0.12 | 0.04 | 0.14 | 0.10 ± 0.05 | | N |
| HD 170357 | 5665 | 4.07 | −0.50 | 1.20 | −0.03 | −0.04 | 0.03 | −0.01 ± 0.04 | T | L |
| | | | | | 0.02 | −0.02 | 0.08 | 0.03 ± 0.05 | | N |
| HD 171620 | 6115 | 4.20 | −0.50 | 1.40 | −0.02 | −0.06 | 0.01 | −0.02 ± 0.04 | D | L |
| | | | | | 0.06 | −0.01 | 0.08 | 0.04 ± 0.05 | | N |
| G 142−2 | 5675 | 4.48 | −0.75 | 1.10 | −0.03 | −0.02 | −0.04 | −0.03 ± 0.01 | T | L |
| | | | | | 0.03 | 0.00 | 0.01 | 0.01 ± 0.02 | | N |
| HD 182807 | 6100 | 4.21 | −0.33 | 1.40 | −0.04 | −0.06 | 0.00 | −0.03 ± 0.03 | D | L |
| | | | | | 0.02 | −0.03 | 0.06 | 0.02 ± 0.05 | | N |
| HD 184448 | 5765 | 4.16 | −0.43 | 1.20 | 0.21 | 0.17 | 0.22 | 0.20 ± 0.03 | T | L |
| | | | | | 0.27 | 0.19 | 0.27 | 0.24 ± 0.05 | | N |
| HD 186379 | 5865 | 3.93 | −0.41 | 1.20 | −0.06 | −0.06 | −0.06 | −0.06 ± 0.00 | D | L |
| | | | | | 0.00 | −0.03 | 0.00 | −0.01 ± 0.02 | | N |
| HD 198300 | 5890 | 4.31 | −0.60 | 1.20 | 0.09 | 0.02 | 0.06 | 0.06 ± 0.04 | T | L |
| | | | | | 0.16 | 0.06 | 0.12 | 0.11 ± 0.05 | | N |
| HD 200580 | 5940 | 3.96 | −0.82 | 1.40 | 0.16 | 0.18 | 0.28 | 0.21 ± 0.06 | ? | L |
| | | | | | 0.28 | 0.26 | 0.39 | 0.31 ± 0.07 | | N |
| G 188−22 | 6040 | 4.37 | −1.25 | 1.50 | −0.54 | −0.46 | ⋯ | −0.50 ± 0.06 | H | L |
| | | | | | −0.39 | −0.36 | ⋯ | −0.38 ± 0.02 | | N |
| HD 201889 | 5710 | 4.05 | −0.78 | 1.10 | −0.11 | −0.17 | −0.13 | −0.14 ± 0.03 | T | L |
| | | | | | −0.03 | −0.13 | −0.06 | −0.07 ± 0.05 | | N |
| HD 204155 | 5815 | 4.09 | −0.66 | 1.20 | −0.02 | 0.00 | 0.02 | 0.00 ± 0.02 | T | L |
| | | | | | 0.06 | 0.04 | 0.09 | 0.06 ± 0.03 | | N |
| HD 208906 | 6025 | 4.37 | −0.76 | 1.40 | −0.07 | −0.09 | −0.02 | −0.06 ± 0.04 | D | L |
| | | | | | 0.02 | −0.04 | 0.06 | 0.01 ± 0.05 | | N |
| G 242−4 | 5815 | 4.31 | −1.10 | 1.20 | −0.52 | −0.44 | −0.40 | −0.45 ± 0.06 | H | L |
| | | | | | −0.42 | −0.39 | −0.30 | −0.37 ± 0.06 | | N |
| HD 215257 | 6030 | 4.28 | −0.58 | 1.40 | −0.18 | −0.22 | −0.14 | −0.18 ± 0.04 | D | L |
| | | | | | −0.11 | −0.18 | −0.08 | −0.12 ± 0.05 | | N |
| HD 218209 | 5665 | 4.40 | −0.60 | 1.10 | 0.14 | 0.09 | 0.17 | 0.13 ± 0.04 | T | L |
| | | | | | 0.20 | 0.11 | 0.22 | 0.18 ± 0.06 | | N |
| HD 221876 | 5865 | 4.29 | −0.60 | 1.20 | −0.07 | −0.07 | 0.05 | −0.03 ± 0.07 | D | L |
| | | | | | 0.00 | −0.04 | 0.11 | 0.02 ± 0.08 | | N |
| HD 224930 | 5480 | 4.45 | −0.66 | 0.90 | −0.16 | −0.16 | −0.15 | −0.16 ± 0.01 | ? | L |
| | | | | | −0.12 | −0.15 | −0.12 | −0.13 ± 0.02 | | N |
| G 69−8 | 5640 | 4.43 | −0.55 | 1.10 | 0.13 | 0.07 | 0.11 | 0.10 ± 0.03 | T | L |
| | | | | | 0.18 | 0.09 | 0.15 | 0.14 ± 0.05 | | N |

**Notes.** Both LTE and non-LTE copper abundances (for each star, first and second rows, respectively) of our program stars are listed in column 9. The abundances given here are the relative values of [Fe/H] derived from Fe2 lines (Section 3.2). Columns 6–8 are the abundances derived from corresponding Cu I lines. The stellar parameters and population assignments are also shown in the table. The characters "D", "T", "H", and "?" in the "POP" column represent thin-disk, thick-disk, halo, and peculiar stars, respectively. The rightmost column indicates the line formation scenario for each star, where "L" represents LTE line formation and "N" represents non-LTE line formation.

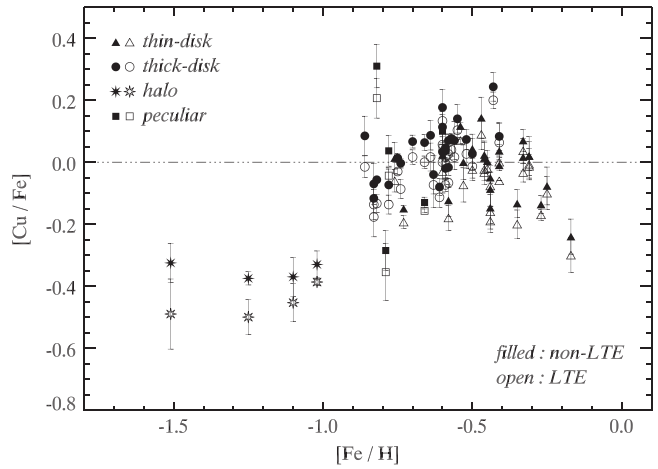


**Figure 3.** Abundance ratios [Cu/Fe] as a function of [Fe/H] for our program stars, where non-LTE and LTE results are represented by filled and open symbols, respectively. Furthermore, symbols with different shapes represent stars from different populations, which are: triangle—thin disk, circle—thick disk, star—halo, square—objects with peculiarities. The errors are evaluated by computing the standard deviations of the abundances derived from different spectral lines.

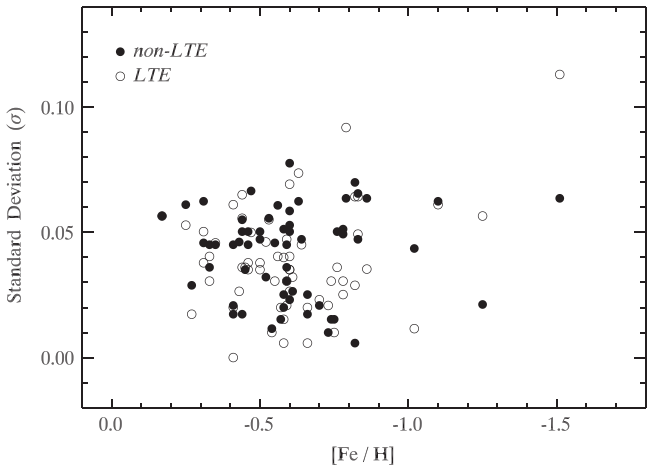


**Figure 4.** Distribution of the standard deviation as a function of metallicity, where filled and open circles represent non-LTE and LTE calculations, respectively. The stars whose copper abundances were derived using only one single line were not plotted in the figure.

magnitudes brighter than 6.5 and distances less than 14.5 pc from the Sun. The spectra were obtained with $R = 50{,}000$ and S/N $> 150$. Compared with their sample, we have only one star in common. The difference in the [Cu/Fe] value is −0.07.

*Nissen & Schuster (2011).* Nissen & Schuster carried out a series of elemental abundance analyses on a sample of 94 dwarfs, most of which were identified as halo stars. They found that the halo stars in the solar neighborhood fall into two distinct populations that can be separated by [$\alpha$/Fe]. They used the 5105, 5218, and 5782 Å lines to derive copper abundances. The log *gf* values adopted in their analyses are similar to those used in ours. Our results are quite consistent with theirs. The average difference is $0.00 \pm 0.05$ for the 11 stars in common.

## 6. DISCUSSION

### 6.1. The Evolutionary Trend of [Cu/Fe] and Nucleosynthesis in the Galaxy

The observational trend of [X/Fe] as a function of [Fe/H] is a powerful tool in revealing the origins of elements and constraining the GCE model. The trend of copper in our Galaxy has been investigated in many papers, but all of the calculations are under LTE assumptions.

Figure 3 displays the results of [Cu/Fe] in our program stars as a function of [Fe/H] for both LTE and non-LTE calculations. The [Cu/Fe] trend is similar to the LTE results of earlier works, but not in the case of non-LTE. In order to show the features more clearly, we present the average [Cu/Fe] values for each 0.1 dex bin of [Fe/H] ($\Delta$[Fe/H] = 0.1 bin) in Figure 7 for non-LTE results. Stars from different populations are averaged separately, and the peculiar stars are not included. The error bars represent the abundance dispersions of the corresponding bins (no bar is plotted if there are only one or two stars in the bin). A flat distribution of [Cu/Fe] can be seen for our non-LTE results in the range of $-1.5 <$ [Fe/H] $< -1.0$, which is different from that revealed by previous works (a linear increase from [Fe/H] = −1.5 to −1.0). However, it should be noted that there are only four stars in that region, and more data are needed to confirm this trend. Even though there may exist bias, the [Cu/Fe] trend derived from non-LTE is still much flatter than that from LTE at $-1.5 <$ [Fe/H] $< -1.0$. The [Cu/Fe] trend for disk stars is not discussed often. Prochaska et al. (2000) studied the copper abundances for 10 thick-disk stars, and a supersolar [Cu/Fe] can be seen in their results at [Fe/H] $\sim -0.4$. Reddy et al. (2006) suggested that the [Cu/Fe] seemed slightly greater for thick-disk stars than for thin-disk stars. Our results indicate that the [Cu/Fe] gradually increases with increasing [Fe/H] for the thick-disk stars, while most of the thin-disk stars have a solar [Cu/Fe] value in the overlapping region. Thus, the thick-disk population appears to have a slight overabundance of [Cu/Fe] at $-0.7 <$ [Fe/H] $< -0.4$.

Several groups (e.g., Matteucci et al. 1993; Timmes et al. 1995; Mishenina et al. 2002; Kobayashi et al. 2006; Romano & Matteucci 2007; Romano et al. 2010) have modeled the GCE of copper. The most difficult part of modeling is to find satisfactory copper abundances at both the metal-poor end and solar metallicity: normal SNe II yields from Woosley & Weaver (1995), case B, give a good estimate of the observed [Cu/Fe] trend for [Fe/H] $> -2$ but lead to overabundant copper at lower metallicities, while the yields from Kobayashi et al. (2006) SNe II mixed with hypernovae give a better fitting in the metal-poor end but fail to reproduce the observational trend at solar metallicity (Romano et al. 2010). The ways to solve this inconsistency are limited because (1) the contribution from the *s*-process cannot be changed freely (Matteucci et al. 1993) and (2) there are still large uncertainties in modeling the yields from low- and intermediate-mass AGB stars or supernova explosion events (Romano & Matteucci 2007; Romano et al. 2010). Since the departures from LTE for Cu I show a clear dependence on metallicity, the copper abundances of the very/extremely metal-poor stars are expected to increase toward lower metallicity (Roederer et al. 2014; J. R. Shi et al. 2014, in preparation). Consequently, before modifying GCE models, a firm and reliable observational trend of [Cu/Fe] should be established first.

### 6.2. The Bending

The non-LTE results for disk stars suggest that there may be a bending-like feature at [Fe/H] $> -1.0$ (Figure 3), where the [Cu/Fe] trend goes up at first but decreases slightly as [Fe/H]

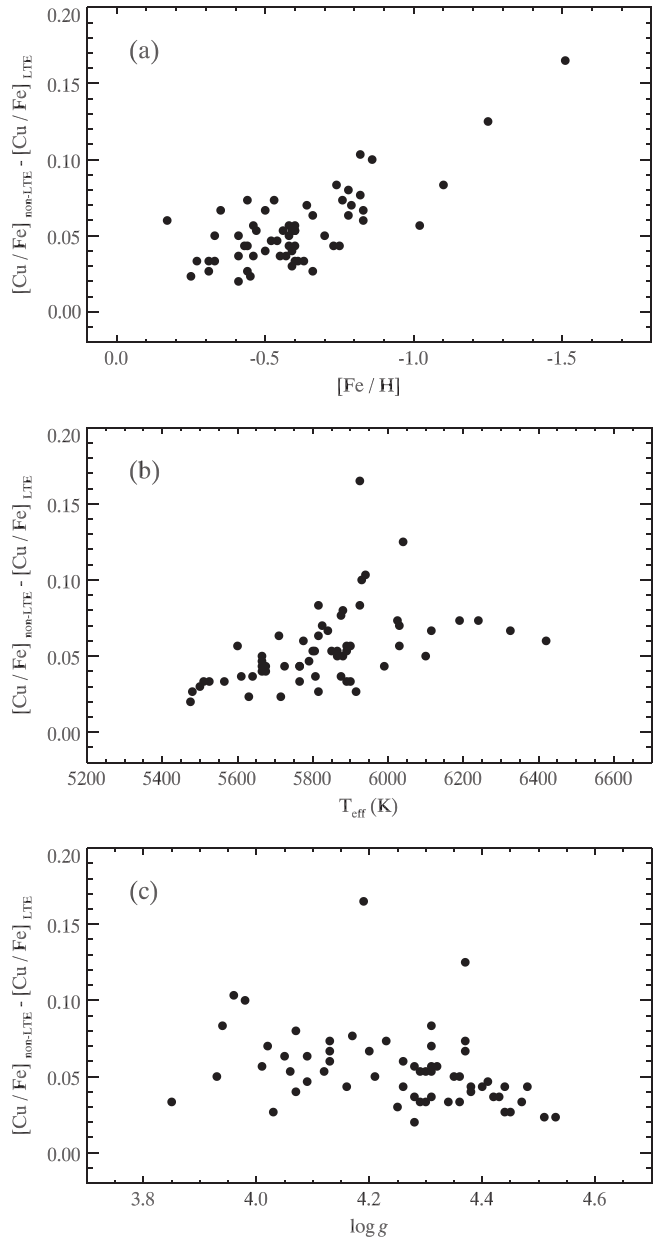


**Figure 5.** Differences in [Cu/Fe] between non-LTE and LTE for our program stars as a function of metallicity (a), effective temperature (b), and surface gravity (c).

becomes higher. The feature can be seen in Figure 7 as well. The term "bending" was introduced by Bisterzo et al. (2004, 2005) and Romano & Matteucci (2007). Those authors superimposed [Cu/Fe] data from different works, and a bending for disk stars appeared in the overlapping region; however, the possibility that the bending may be caused by a systematic offset between different studies could not be ruled out. A similar feature can be found for our non-LTE results, and it should be noted that we do not have enough data at [Fe/H] $> -0.3$; the decline in this region is mainly produced by three stars, and as a result, more data are needed to draw a firm conclusion.

One of the explanations for the bending might be SNe Ia. However, the typical timescale for chemical enrichment from SNe Ia in the Milky Way is model-dependent (e.g., Matteucci & Recchi 2001) and thus not strictly constrained.

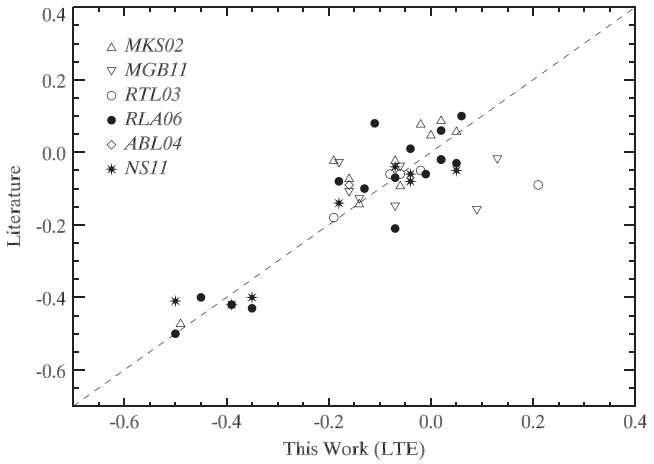


**Figure 6.** Comparison of derived [Cu/Fe] in the LTE analysis of the stars in common with the literature, including MKS02 (Mishenina et al. 2002), MGB11 (Mishenina et al. 2011), RTL03 (Reddy et al. 2003), RLA06 (Reddy et al. 2006), ABL04 (Allende Prieto et al. 2004), and NS11 (Nissen & Schuster 2011). Corresponding symbols are annotated in the figure.

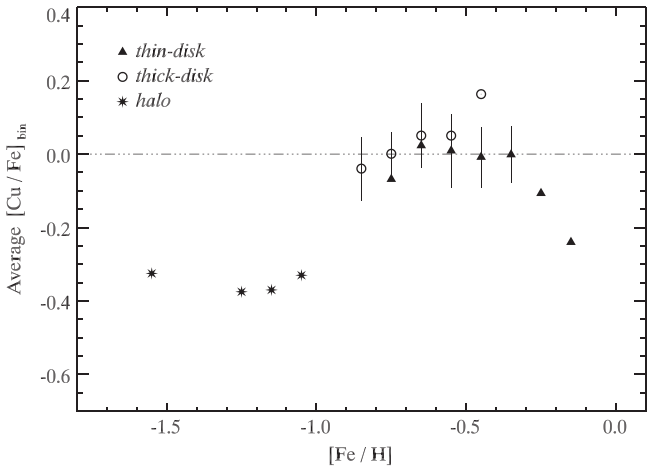


**Figure 7.** Trend of average [Cu/Fe] for the 0.1 dex bin of [Fe/H]; only non-LTE results are presented. Stars from different populations are averaged separately, and the peculiar stars are not included. The error bars represent the abundance dispersions of the corresponding bins.

## 7. CONCLUSIONS

We have investigated the copper abundances for 64 late-type stars with effective temperatures from 5400 to 6700 K and [Fe/H] between −1.88 and −0.17. Non-LTE statistical equilibrium calculations are performed to derive the copper abundances. Based on our results, we come to the following conclusions.

1. Non-LTE effects are significantly large for copper, and they differ from line to line. Two Cu I lines, 5105 Å and 5782 Å, are more sensitive to non-LTE effects. The non-LTE corrections for these lines can reach ∼0.2 dex at a metallicity of [Fe/H] $\sim -1.5$. The weaker line, 5218 Å, shows relatively small but still not negligible non-LTE effects, with a maximum departure of 0.13 dex in our sample.
2. The copper abundances are underestimated in LTE calculations. Taking non-LTE effects into account, the copper abundances increase for all of our program stars.
3. The non-LTE effects clearly show a dependence on metallicity, and they increase with decreasing [Fe/H].

4. Our non-LTE results show that there might be a [Cu/Fe] plateau in the metallicity range $-1.5 < [Fe/H] < -1.0$; however, we need more data to confirm this result. The thick- and thin-disk stars might have different behaviors in [Cu/Fe], and a bending of the disk stars may exist.

Further non-LTE studies of copper abundance in various environments with a wider metallicity range need to be carried out. They are essential to understanding the origination and evolution of copper.

This research was supported by the National Natural Science Foundation of China under grant Nos. 11321064, 11233004, 11390371, 11473033, U1331122, and by National Key Basic Research Program of China 2014CB845700.

## REFERENCES


Ali, A. W., & Griem, H. R. 1966, PhRv, 144, 366
Allen, C. W. 1973, Astrophysical Quantities (3rd ed.; London: Athlone)
Allende Prieto, C., Barklem, P. S., Lambert, D. L., & Cunha, K 2004, A&A, 420, 183
Anstee, S. D., & O'Mara, B. J. 1991, MNRAS, 253, 549
Anstee, S. D., & O'Mara, B. J. 1995, MNRAS, 276, 859
Asplund, M., Grevesse, N., Sauval, A. J., & Scott, P. 2009, ARA&A, 47, 481
Baumueller, D., & Gehren, T. 1997, A&A, 325, 1088
Baumueller, D., Butler, K., & Gehren, T. 1998, A&A, 338, 637
Bergemann, M., & Gehren, T. 2008, A&A, 492, 823
Biehl, D. 1976, PhD thesis, University of Kiel
Bihain, G., Israelian, G., Rebolo, R., Bonifacio, P., & Molaro, P. 2004, A&A, 423, 777
Bisterzo, S., Gallino, R., Pignatari, M., et al. 2004, MmSAI, 75, 741
Bisterzo, S., Pompeia, L., Gallino, R., et al. 2005, NuPhA, 758, 284
Bonifacio, P., Caffau, E., & Ludwig, H.-G. 2010, A&A, 524, A96
Butler, K., & Giddings 1985, J. Newsletter on the Analysis of Astronomical Spectra No. 9
Castro, S., Porto de Mello, G. F., & da Silva, L. 1999, MNRAS, 305, 693
Cohen, J. G. 1978, ApJ, 223, 487
Cohen, J. G. 1979, ApJ, 231, 751
Cohen, J. G. 1980, ApJ, 241, 981
Cohen, J. G., Christlieb, N., McWilliam, A., et al. 2008, ApJ, 672, 320
Cowan, J. J., Sneden, C., Burles, S., et al. 2002, ApJ, 572, 861
Cunha, K., Smith, V. V., Suntzeff, N. B., et al. 2002, AJ, 124, 379
Drawin, H. W. 1968, ZPhy, 211, 404
Drawin, H. W. 1969, ZPhy, 225, 483
Gehren, T., Liang, Y. C., Shi, J. R., Zhang, H. W., & Zhao, G. 2004, A&A, 413, 1045
Gehren, T., Shi, J. R., Zhang, H. W., Zhao, G., & Korn, A. J. 2006, A&A, 451, 1065
Gratton, R. G., & Sneden, C. 1988, A&A, 204, 193
Grupp, F. 2004, A&A, 420, 289
Grupp, F., Kurucz, R. L., & Tan, K. 2009, A&A, 503, 177
Gurtovenko, E. A., & Kostyk, R. I. 1989, KiIND, 200
Kobayashi, C., Umeda, H., Nomoto, K., Tominaga, N., & Ohkubo, T. 2006, ApJ, 653, 1145
Kurucz, R. L. 2009, http://kurucz.harvard.edu/atoms/2600/, http://kurucz.harvard.edu/atoms/2601/,http://kurucz.harvard.edu/atoms/2602/
Lai, D. K., Bolte, M., Johnson, J. A., et al. 2008, ApJ, 681, 1524
Liu, Y. P., Gao, C., Zeng, J. L., Yuan, J. M., & Shi, J. R. 2014, ApJS, 211, 30
Lodders, K., Palme, H., & Gail, H. P. 2009, in Landolt-Börnstein, Vol. 6/4B, ed. J. E. Trumper (Berlin: Springer), 560
Mashonkina, L., Gehren, T., Shi, J.-R., Korn, A. J., & Grupp, F. 2011, A&A, 528, A87
Matteucci, F., Raiteri, C. M., Busson, M., Gallino, R., & Gratton, R. 1993, A&A, 272, 421
Matteucci, F., & Recchi, S. 2001, ApJ, 558, 351
McWilliam, A., & Smecker-Hane, T. A. 2005, ApJL, 622, L29
McWilliam, A., Wallerstein, G., & Mottini, M. 2013, ApJ, 778, 149
Mishenina, T. V., Gorbaneva, T. I., Basak, N. Y., Soubiran, C., & Kovtyukh, V. V. 2011, ARep, 55, 689
Mishenina, T. V., Kovtyukh, V. V., Soubiran, C., Travaglio, C., & Busso, M. 2002, A&A, 396, 189
Nissen, P. E., & Schuster, W. J. 2011, A&A, 530, A15
Nomoto, K., Tominaga, N., Umeda, H., Kobayashi, C., & Maeda, K. 2006, NuPhA, 777, 424
Pfeiffer, M. J., Frank, C., Baumueller, D., Fuhrmann, K., & Gehren, T. 1998, A&AS, 130, 381
Pignatari, M., Gallino, R., Heil, M., et al. 2010, ApJ, 710, 1557
Prochaska, J. X., Naumov, S. O., Carney, B. W., McWilliam, A., & Wolfe, A. M. 2000, AJ, 120, 2513
Reddy, B. E., Lambert, D. L., & Allende Prieto, C. 2006, MNRAS, 367, 1329
Reddy, B. E., Tomkin, J., Lambert, D. L., & Allende Prieto, C. 2003, MNRAS, 340, 304
Reetz, J. K. 1991, Diploma thesis, Universität München
Roederer, I. U., Lawler, J. E., Sobeck, J. S., et al. 2012, ApJS, 203, 27
Roederer, I. U., Schatz, H., Lawler, J. E., et al. 2014, ApJ, 791, 32
Romano, D., & Matteucci, F. 2007, MNRAS, 378, L59
Romano, D., Karakas, A. I., Tosi, M., & Matteucci, F. 2010, A&A, 522, A32
Seaton, M. J. 1962, in Atomic and Molecular Processes (New York: Academic), 374
Shetrone, M. D., Côté, P., & Sargent, W. L. W. 2001, ApJ, 548, 592
Shetrone, M., Venn, K. A., Tolstoy, E., et al. 2003, AJ, 125, 684
Shi, J. R., Gehren, T., & Zhao, G. 2004, A&A, 423, 683
Shi, J. R., Gehren, T., Mashonkina, L., & Zhao, G. 2009, A&A, 503, 533
Shi, J. R., Gehren, T., Zeng, J. L., Mashonkina, L., & Zhao, G. 2014, ApJ, 782, 80
Simmerer, J., Sneden, C., Ivans, I. I., et al. 2003, AJ, 125, 2018
Smith, V. V., Suntzeff, N. B., Cunha, K., et al. 2000, AJ, 119, 1239
Sneden, C., Cowan, J. J., Lawler, J. E., et al. 2003, ApJ, 591, 936
Sneden, C., & Crocker, D. A. 1988, ApJ, 335, 406
Sneden, C., Gratton, R. G., & Crocker, D. A. 1991, A&A, 246, 354
Steenbock, W., & Holweger, H. 1984, A&A, 130, 319
Sugar, J., & Musgrove, A. 1990, JPCRD, 19, 527
Timmes, F. X., Woosley, S. E., & Weaver, T. A. 1995, ApJS, 98, 617
Travaglio, C., Gallino, R., Arnone, E., et al. 2004, ApJ, 601, 864
van Regemorter, H. 1962, ApJ, 136, 906
VandenBerg, D. A., Swenson, F. J., Rogers, F. J., Iglesias, C. A., & Alexander, D. R. 2000, ApJ, 532, 430
Westin, J., Sneden, C., Gustafsson, B., & Cowan, J. J. 2000, ApJ, 530, 783
Woosley, S. E., & Weaver, T. A. 1995, ApJS, 101, 181
Zhao, G., Butler, K., & Gehren, T. 1998, A&A, 333, 219
Zhao, G., & Gehren, T. 2000, A&A, 362, 1077